Meteoritics & Planetary Science 41, Nr 6, 819–833 (2006)
Abstract available online at http://meteoritics.org

Confirmation of a meteoritic component in impact-melt rocks of the Chesapeake Bay impact structure, Virginia, USA—Evidence from osmium isotopic and PGE systematics

Seung Ryeol LEE[1, 3], J. Wright HORTON Jr.[2], and Richard J. WALKER[1*]

[1]Isotope Geochemistry Laboratory, Department of Geology, University of Maryland, College Park, Maryland 20742, USA
[2]U.S. Geological Survey, 926A National Center, 12201 Sunrise Valley Drive, Reston, Virginia 20192, USA
[3]Geology and Geoinformation Division, Korea Institution of Geoscience and Mineral Resources, Daejeon 305-350, South Korea
*Corresponding author. E-mail: rjwalker@geol.umd.edu

(Received 23 November 2005; revision accepted 25 March 2006)

Abstract–The osmium isotope ratios and platinum-group element (PGE) concentrations of impact-melt rocks in the Chesapeake Bay impact structure were determined. The impact-melt rocks come from the cored part of a lower-crater section of suevitic crystalline-clast breccia in an 823 m scientific test hole over the central uplift at Cape Charles, Virginia. The $^{187}Os/^{188}Os$ ratios of impact-melt rocks range from 0.151 to 0.518. The rhenium and platinum-group element (PGE) concentrations of these rocks are 30–270× higher than concentrations in basement gneiss, and together with the osmium isotopes indicate a substantial meteoritic component in some impact-melt rocks. Because the PGE abundances in the impact-melt rocks are dominated by the target materials, interelemental ratios of the impact-melt rocks are highly variable and nonchondritic. The chemical nature of the projectile for the Chesapeake Bay impact structure cannot be constrained at this time. Model mixing calculations between chondritic and crustal components suggest that most impact-melt rocks include a bulk meteoritic component of 0.01–0.1% by mass. Several impact-melt rocks with lowest initial $^{187}Os/^{188}Os$ ratios and the highest osmium concentrations could have been produced by additions of 0.1%–0.2% of a meteoritic component. In these samples, as much as 70% of the total Os may be of meteoritic origin. At the calculated proportions of a meteoritic component (0.01–0.1% by mass), no mixtures of the investigated target rocks and sediments can reproduce the observed PGE abundances of the impact-melt rocks, suggesting that other PGE enrichment processes operated along with the meteoritic contamination. Possible explanations are 1) participation of unsampled target materials with high PGE abundances in the impact-melt rocks, and 2) variable fractionations of PGE during syn- to post-impact events.

INTRODUCTION

Subsequent to the Cretaceous-Tertiary (K/T) impact, the Late Eocene epoch is recognized as having the greatest recorded number of meteorite impacts. These impacts are manifested by the 100 km-diameter Popigai crater in Russia (Whitehead et al. 2000), and the 85 km-diameter Chesapeake Bay structure in the U.S., with respective ages of 35.7 ± 0.8 Ma (Bottomley et al. 1997) and 35.3 ± 0.2 Ma (2σ, Horton and Izett 2005). Three smaller impact craters of comparable age in Mistastin, Canada (38 ± 4 Ma, 28 km; Farley et al. 1998); Wanapitei, Canada (37 ± 2 Ma, 7.5 km; Winzer et al. 1976); and Logoisk, Belarus (40 ± 5 Ma, 17 km; Masaitis et al. 1980) may be linked to the larger impact events. All of these impacts have ages near the peak of a putative Late Eocene comet shower that was proposed by Farley et al. (1998) on the basis of a marked enhancement of interplanetary dust particle flux to marine sediments. The putative event may have played an important role related to the deterioration of the global climate at the end of the Eocene epoch (Bodiselitsch et al. 2004). The comet shower hypothesis, however, is in conflict with an asteroidal collision hypothesis proposed by Tagle and Claeys (2004, 2005). On the basis of the elemental ratios of certain platinum-group elements (PGE) in the impact-melt rocks of the Popigai crater, they argued that the projectile at Popigai was an asteroid of L-chondrite composition rather than a comet. Therefore, identification of the projectile involved in the Late Eocene Chesapeake Bay impact structure (CBIS) may provide more information about the nature of the Late Eocene impactors

and whether they are related to a comet or asteroid shower. Background information on the CBIS is available in Koeberl et al. (1996), Powars and Bruce (1999), Powars (2000), Poag et al. (2004), and Horton et al. (2005a).

Small impact craters commonly retain physical remnants of the impacting body (or projectile), thus readily establishing their impact origin (Grieve 1991). However, during the formation of larger craters (>~1.5 km in diameter), the projectile is generally vaporized and destroyed as a physical entity by the enormous temperatures and shock pressures generated during impact (Grieve 1991; Koeberl and Shirey 1997). During the early stage of an impact event, high-speed ejecta remove the bulk of the projectile mass from the immediate region of the crater (O'Keefe and Ahrens 1987). Only a small amount of the finely dispersed meteoritic melt droplets or vapor is mixed with a much larger quantity of target-derived vapor and melt in impact-melt rock, melt breccia, and impact glass deposits (Koeberl and Shirey 1997; Koeberl et al. 2004).

Because target materials typically make up >99% of impact-melt rocks, it can be difficult to decipher the compositional characteristics of the projectile from those of the target (Koeberl 1998). Identification of the chemical nature of projectiles mostly has been achieved by the study of the concentrations and interelemental ratios of siderophile elements, especially PGE (e.g., Morgan et al. 1979; Palme et al. 1979, 1981; Wolf et al. 1980; Evans et al. 1993; Schmidt et al. 1997; Tagle and Claeys 2004, 2005). The PGE have been emphasized because their abundances in chondrites are several orders of magnitude higher than in most terrestrial crustal rocks. Previous studies have revealed a variety of projectile types, encompassing a wide range of known meteorite compositions (Grieve 1991). In some impact structures, the identification of the impactor, based on the relative abundances of PGE, has been hampered for a variety of reasons, including variations in concentrations in target rock, mobility and the concentration of PGE by purely terrestrial processes, and fractionation during the impact process (Colodner et al. 1992; Sawlowicz 1993; Evans and Chai 1997; Koeberl and Shirey 1997; Schmitz et al. 2004). In such cases, the rhenium-osmium (Re-Os) isotope system ($^{187}Re \rightarrow {}^{187}Os + \beta^-$; $\lambda = 1.67 \times 10^{-11} a^{-1}$) has served as a complement to PGE concentrations (Koeberl and Shirey 1993; Meisel et al. 1995; Gelinas et al. 2004). Like Ir, Os is normally highly enriched in meteoritic projectiles relative to crustal rocks (e.g., Koeberl and Shirey 1997; Koeberl et al. 2002). For example, chondrites contain 400–800 ppb Os, while most terrestrial crustal rocks (except peridotites) contain <0.05 ppb Os (e.g., Morgan and Lovering 1967). Of greater importance is that the Os isotopic composition ($^{187}Os/^{188}Os$ ratio) of crustal rocks, especially continental crust, normally is more radiogenic (higher) than likely projectiles. The $^{187}Os/^{188}Os$ ratios of most primitive meteorites average about 0.13, whereas continental crustal rocks average about 1.0–1.4 (e.g., Esser and Turekian 1993; Peucker-Ehrenbrink and Jahn 2001). Thus, even the addition of a minor (<<1%) meteoritic component to terrestrial rocks can result in a major change in the $^{187}Os/^{188}Os$ values of the mixture (Koeberl and Shirey 1997).

The purpose of this study is 1) to test for the presence of a meteoritic component in the CBIS on the basis of Re-Os isotopic and PGE data from the impact-melt rocks in the crater, 2) to constrain the proportions of the meteoritic component in various impact-melt rocks, 3) to determine the origin of Re and PGE budgets in the impact-melt rocks, and 4) to attempt to infer the projectile type by using interelemental PGE ratios. As far as we know, this is the first real teaming of osmium isotopes and a full range of PGE in a study of this kind.

SAMPLES

The impact-melt rocks sampled in this study come from the cored part of a lower crater section of suevitic crystalline-clast breccia in an 823 m scientific test hole over the central uplift at Cape Charles, Virginia (Fig. 1). As described by Sanford et al. (2004) and Horton et al. (2004, 2005b), the stratigraphic section in the test hole consists of three parts: 1) a lower-crater section of crystalline-clast breccia and brecciated gneiss, 2) an upper-crater section of unconsolidated sediment-clast breccia, and 3) post-impact unconsolidated sediments. The cored part of the lower crystalline-clast breccia is largely suevitic, and it contains metamorphic and igneous rock fragments and less abundant pieces of impact-melt rock. The suevitic crystalline-clast breccia and its contained fragments in the Cape Charles test hole show petrographic evidence for pervasive post-impact hydrothermal chloritization and albitization (Horton et al. 2005b; Sanford 2005), which are not observed in drill cores from the outer parts of the structure (Horton et al. 2005a).

Seven samples of impact-melt rock (ST2440.8C, ST2453.3C, ST2470.6C, ST2565.0C, ST2567.6C, ST2570.0C, and ST2582.1C) were collected from clasts in the suevitic crystalline-clast breccia (Table 1). Additional samples of breccia that contain impact melt as well as gneiss fragments (similar to sample STP2-1 below) include a matrix portion of suevitic breccia (ST2562.8C, <50% melt rock) and impact-melt breccia (ST2570.9C, >50% melt rock) from a local occurrence within the suevitic breccia. A clast of reworked, altered impact-melt rock (UN749.4) from a sedimentary breccia (Exmore beds) in the USGS North corehole (Fig. 1) was also sampled.

Seven samples of rocks and sediments representative of the pre-impact target were sampled for analysis to determine the indigenous Re and PGE concentrations for comparison with the impact-melt rocks. These samples of target materials include quartzofeldspathic gneiss (STP2-1) from a megablock in the suevitic crystalline-clast breccia at Cape Charles and a

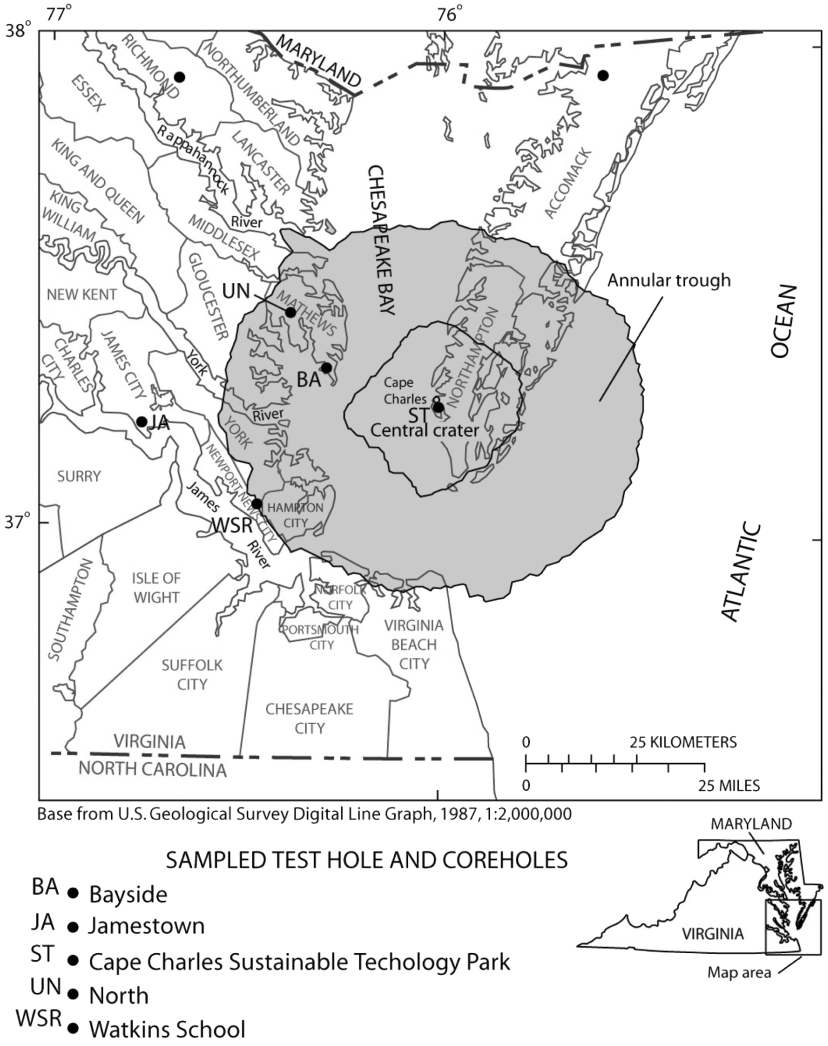

Fig. 1. A map showing the Chesapeake Bay impact structure and sample localities in southeastern Virginia. Samples of impact-melt rock, and breccias that contain impact-melt rock, come from a scientific test hole on the central uplift (ST, USGS Cape Charles Sustainable Technology Park test hole, Northampton, Co., Virginia.). Other samples, including pre-impact target materials, come from this test hole and from other coreholes in and near the annular trough: BA = USGS Bayside corehole (Mathews Co., Virginia), JA = Jamestown corehole (James City Co., Virginia), UN = USGS North corehole (Mathews Co., Virginia), WSR = USGS Watkins School corehole (Newport News, Virginia). Locations of the central crater and outer margin are from Powars and Bruce (1999). Modified from Horton et al. (2005c, Fig. A1).

brecciated metamafic rock (ST2672.3C) interpreted to be a pre-impact intrusive into the gneiss. The gneiss and metamafic rock are presently interpreted as parts of a megablock that became mixed into the fallback suevite, possibly during the central-uplift rise and collapse; the gneiss has a sensitive high-resolution ion microprobe (SHRIMP) U-Pb zircon age of 612 ± 8 Ma (2σ, Horton et al. 2005b). A Neoproterozoic monzogranite (BA2372), Cretaceous nonmarine clay (WSR674.1) and sand (WSR728.7), an upper Paleocene glauconite-bearing sand (JA2), and a Middle Eocene limestone (JA7) also were analyzed in order to investigate other possible target-material contributions to the impact melt (Table 1). These samples come from several coreholes in and near the annular trough of the CBIS (Table 1 and Fig. 1).

ANALYTICAL METHODS

Samples were ground to fine powder using a ceramic mortar and pestle. Approximately 0.1–2.0 g of powder, along with separate ^{187}Re and ^{190}Os spikes, and a mixed PGE spike consisting of ^{99}Ru, ^{105}Pd, ^{191}Ir, and ^{194}Pt, were digested in Carius tubes in reverse aqua regia at 230 °C for at least 2 days (Shirey and Walker 1995). Subsequent separation/purification was accomplished by solvent extraction (Os) and anion exchange chromatography (Re, Ru, Pd, Ir, and Pt). Osmium analysis was accomplished by negative thermal ionization mass spectrometry using the University of Maryland Bobcat I mass spectrometer. The remaining PGE and Re were analyzed using the University of Maryland Nu Plasma multi-collector ICP-MS with electron multiplier detectors. Instrumental mass

Table 1. Sources and descriptions of impact-melt rocks and target materials sampled in this study.

Sample	Locality[a]	Depth in feet[b]	Lithologic description
Pre-impact target materials (rocks and sediments)			
Marine sediments (Tertiary)			
JA2	JA	242.7–243.0	Quartz-glauconite sand, silty, black to greenish black, mostly fine sand; Aquia Formation (upper Paleocene), Piscataway member, marine.
JA7	JA	242.7–243.0	Limestone (mollusk wackestone), light gray, fine-grained; Piney Point Formation (Middle Eocene), marine.
Non-marine sediments (Cretaceous)			
WSR674.1	WSR	674.1–674.4	Silty clay, pale reddish brown; Potomac Formation (Cretaceous).
WSR728.7	WSR	728.7–729.0	Feldspathic quartz sand, silty, yellowish gray; mostly fine sand; Potomac Formation (Cretaceous).
Crystalline basement rocks (pre-Mesozoic)			
STP2-1	ST	2682.3–2684.5	Quartzofeldspathic gneiss (Neoproterozoic) from megablock in suevitic breccia; light gray, fine to medium grained, thinly layered and variably brecciated.
ST2672.3C	ST	2672.3–2672.7	Metamafic rock (age undetermined); massive, medium gray, aphanitic, nonfoliated, chloritized and albitized; pre-impact intrusive into gneiss from megablock in suevitic breccia, variably brecciated.
BA2372	BA	2370.8–2373.5	Granite at Bayside (Neoproterozoic); pale red, leucocratic monzogranite with partly chloritized biotite; beneath annular trough
Impact-melt rocks (clasts in suevitic breccia)			
ST2440.8C	ST	2440.8–2441.0	Impact-melt rock, dark greenish gray, aphanitic to partly hyaline; dike within a gneissic block in suevitic breccia.
ST2453.3C	ST	2453.3–2453.7	Holocrystalline mafic rock, grayish-black, aphanitic, and nonfoliated; part of block in suevitic breccia.
ST2470.6C	ST	2470.6–2470.7	Impact-melt rock, medium-gray, flow laminated; clast in suevitic breccia.
ST2565.0C	ST	2565.0–2565.1	Impact-melt rock, greenish gray, flow laminated; clast in suevitic breccia
ST2567.6C	ST	2567.6–2567.7	Impact-melt rock, medium light gray, aphanitic, flow laminated; clast in suevitic breccia.
ST2570.0C	ST	2570.0	Impact-melt rock, brownish-gray, flow laminated, aphanitic to partly hyaline; flow-laminated bomb (fladen) in suevitic breccia.
ST2582.1C	ST	2582.1	Impact-melt rock, medium dark gray, massive; clast in suevitic breccia.
Breccias that contain impact-melt rock			
ST2562.8C	ST	2562.8–2563.0	Suevitic breccia matrix containing bits of flow-laminated melt rock and cataclastic gneiss.
ST2570.9C	ST	2570.9	Impact-melt breccia, medium light gray, fine-grained, clast-rich; in suevitic breccia as tabular zone.
Reworked impact-melt clast			
UN749.4	UN	749.3–749.5	Altered impact-melt rock, light olive gray, flow laminated and vesicular; reworked clast in sedimentary breccia (Exmore beds).

[a]Localities (see Fig. 1): BA = USGS Bayside corehole (Mathews Co., Virginia), JA = Jamestown corehole (James City Co., Virginia), ST = USGS Cape Charles Sustainable Technology Park test hole (Northampton Co., Virginia), UN = USGS North corehole (Mathews Co., Virginia), WSR = USGS Watkins School core-hole (Newport News, Virginia).

[b]Cores were originally measured and labeled in tenths of feet.

fractionations for Re, Ir, Ru, Pt, and Pd were linearly corrected using $^{185}Re/^{187}Re = 0.5975$, $^{191}Ir/^{193}Ir = 0.5949$, $^{99}Ru/^{101}Ru = 0.7479$, $^{194}Pt/^{196}Pt = 1.306$, and $^{105}Pd/^{106}Pd = 0.8170$ relative to those measured in the standard solution that was run interspersed with samples. Additional details regarding chemical separations and mass spectrometry can be found in Walker et al. (2002) and Horan et al. (2003). Blanks for Re, Os, Ir, Ru, Pt, and Pd averaged 3.9 (±1.6), 2.1 (±0.3), 3.1 (±1.2), 33 (±12), 31 (±4), and 36 (±10) pg, respectively, where $n = 5$. The $^{187}Os/^{188}Os$ ratio of the blank had an average of 0.17 (±0.01). In-run statistics for measurements of $^{187}Os/^{188}Os$ were better than ±0.3% (2σ). Because of the range in the quantities of highly siderophile elements (HSE) present among the samples, uncertainties in the abundance data are highly variable, with the magnitude of uncertainties largely reflecting blank/sample ratios. For samples with relatively high Os contents (>10 pg), uncertainties are ±0.3–2.5% for $^{187}Os/^{188}Os$ isotopic composition and ±0.3–3% for Os concentration, respectively. For samples with relatively low Os contents (<10 pg), uncertainties are approximately 0.3–53% for $^{187}Os/^{188}Os$ isotopic composition and 6–25% for Os concentration, respectively. The $^{187}Re/^{188}Os$ ratios for all samples are variable, so corrections for 36 Ma of ^{187}Os ingrowth vary from 0.1% to 17%.

Uncertainties in Re concentrations are better than 4% for all but five samples (WSR674.1, STP2-1, BA2372, ST2470.6C, and ST2567.6C), which have relatively high uncertainties of 12–21% due to high blank/sample ratios. Uncertainties in Ir, Ru, Pt, and Pd concentrations of all the impact-melt rocks are approximately 0.3–6%, 0.1–20%, 0.2–4%, and 0.2–5%, respectively. Because of low PGE contents, however, uncertainties in Ir, Ru, Pt, and Pd of various target rocks are generally greater, ranging between 8–41%, 20–44%, 6–48% and 8–50%, respectively, largely due to high blank/sample ratios.

RESULTS

Target Rocks and Sediments

Rhenium and PGE concentrations and Re-Os isotopic data of the target materials and impact-melt rocks are given in Table 2. The Ru quantities for samples JA2, ST2672.3C, and BA2372, and the Pd quantity for sample BA2372, were at blank levels (below detection), so concentrations are not reported.

Rhenium and PGE concentrations of quartzofeldspathic gneiss sample STP2-1, which typifies the most common target-rock fragments in suevitic breccia that also contains the impact-melt rocks, are 0.004 ppb Re, 0.004 ppb Os, 0.004 ppb Ir, 0.009 ppb Ru, 0.038 ppb Pt, and 0.053 ppb Pd. These concentrations are approximately 50, 8, 6, 23, 13, and 10 times lower, respectively, than the estimated average upper continental crust (UCC) (Re = 0.198 ppb, Os = 0.031 ppb, Ir = 0.022 ppb, Ru = 0.21 ppb, Pt = 0.51 ppb, Pd = 0.52 ppb; Peucker-Ehrenbrink and Jahn 2001). The chondrite normalized Re-PGE pattern of the gneiss is broadly similar to that of the UCC (Fig. 2a). The calculated initial $^{187}Os/^{188}Os$ ratio for 36 Ma is 4.62 (γ_{Os} = +3540; where γ_{Os} is the percent deviation of the $^{187}Os/^{188}Os$ ratio from a chondritic average at the time of comparison), indicative of very radiogenic Os in the gneiss at the time of impact.

The PGE concentrations of duplicate aliquots of metamafic rock sample ST2672.3C are similar to that of the quartzofeldspathic gneiss, although with Re concentrations that are significantly higher; PGE concentrations are more comparable to the UCC average. Due to the high Re concentrations in the metamafic rock, its $^{187}Re/^{188}Os$ ratios (340–571) are also significantly higher than the gneiss (6.17), but $^{187}Os/^{188}Os$ ratios (4.47 and 5.13) are similar to that of the gneiss. The difference between duplicate analyses of the same powder likely results from the unequal distribution of Re and PGE among aliquots due to the nugget effect.

Granite sample BA2372 was recovered from a corehole that was drilled through the entire crater-fill section into the underlying crystalline basement in the annular trough. It has a Neoproterozoic SHRIMP U-Pb zircon age of 625 ± 11 Ma (2σ; Horton et al. 2002), which is similar to the age of the quartzofeldspathic gneiss. The Re and Os concentrations of the granite are 0.018 ppb and 0.022 ppb, respectively, approximately five times higher than the gneiss, but other PGE concentrations are generally low (below the detection limit for Ru and Pd). Although $^{187}Re/^{188}Os$ ratios for both the granite and gneiss are similarly low, the initial $^{187}Os/^{188}Os$ ratio of the granite is significantly lower than that of the gneiss (0.155, γ_{Os} = +22).

Rhenium, Os, Ir, and Ru concentrations of Cretaceous unconsolidated nonmarine sediment samples WSR674.1 (clay) and WSR728.7 (sand) are generally enriched in PGE relative to the gneiss but depleted relative to the UCC average. Except for relative enrichments in Pt and Pd, the overall Re-PGE patterns of these sediments are similar to that of the gneiss (Fig. 2a). The $^{187}Re/^{188}Os$ ratios for samples WSR674.1 and WSR728.7 are 3.42 and 18.4, respectively, similar to the gneiss, but $^{187}Os/^{188}Os$ ratios are 0.9825 (γ_{Os} = +675) and 0.8517 (γ_{Os} = +572), respectively, much lower than that of the gneiss.

The uppermost target units examined here, an upper Paleocene glauconitic sand (JA2) and a Middle Eocene limestone (JA7) are marine sediments that are lithologically and chemically distinct from the other target sediments and rocks. They are characterized by significant enrichments in Re and Os. Rhenium and Os concentrations of these sediments range from 3.64 to 5.64 ppb and from 0.125 to 0.248 ppb, respectively (Table 2). In contrast, other PGE concentrations are similar to those of the two Cretaceous sediments (Figs. 2a and 2b). The enrichments in Re and Os present in JA2 and JA7 can be attributed to their Fe-rich and organic-rich natures. Due to their high Re, $^{187}Re/^{188}Os$ ratios are variably high (73.9 and 237), but $^{187}Os/^{188}Os$ ratios are relatively low (0.4176 and 0.7198, γ_{Os} = +229 and +468) compared to all of the other target materials except the granite (BA2372).

Impact-Melt Rocks

With one exception (sample ST2565.0C which has low Os and Ir concentrations), all of the analyzed impact-melt rocks are enriched by factors of 30–270 in Re and PGE relative to the gneiss (STP2-1). Moreover, the degree of enrichment is similar for each element. The PGE concentrations in most of the impact-melt rocks are also higher than those of the average UCC (Peucker-Ehrenbrink and Jahn 2001) (Fig. 2c). The chondrite normalized Re-PGE patterns of the impact-melt rocks are similar to those of the gneiss and other target rocks (Figs. 2a and 2c), but have proportionally higher Ru, Pt, and Pd.

Compared to the target rocks, the $^{187}Re/^{188}Os$ ratios of all the impact-melt rocks (except for the low-Os sample ST2565.0C) are restricted to a relatively narrow range of 1.13–8.16. Exempting the anomalous sample ST2565.0C, initial $^{187}Os/^{188}Os$ ratios also have a narrow range of 0.1480–

Table 2. Re-Os isotopic compositions and PGE concentrations (in ppb) of impact-melt rocks and target materials (rocks and sediments) from the Chesapeake Bay impact structure.

Sample[a]	Wt. (g)	Re	Os	Ir	Ru	Pt	Pd	$^{187}Re/^{188}Os$	$^{187}Os/^{188}Os$	2σ	$^{187}Os/^{188}Os_{(T = 36\ Ma)}$	$\gamma_{Os\ (T=36Ma)}$[b]
Pre-impact target materials (rocks and sediments)												
JA2 (glauconitic sand)	2.09	3.64	0.248	0.029	b.d.[c]	0.241	0.155	73.9	0.4690	0.0004	0.4246	235
JA2-duplicate	2.02	4.24	0.247	0.032	b.d.	0.262	0.140	86.3	0.4693	0.0005	0.4176	229
JA7 (limestone)	0.50	5.64	0.125	0.007	0.037	0.114	0.040	237	0.8622	0.0024	0.7198	468
WSR674.1 (clay)	2.06	0.008	0.012	0.023	0.030	0.857	1.31	3.42	0.9846	0.0016	0.9825	675
WSR728.7 (sand)	2.02	0.031	0.009	0.010	0.027	0.369	0.233	18.4	0.8628	0.0016	0.8517	572
STP2-1 (felsic gneiss)	2.07	0.004	0.004	0.004	0.009	0.038	0.053	6.17	4.620	0.0090	4.616	3540
ST2672.3C (metamafic)	1.99	0.186	0.004	0.002	b.d.	0.038	0.123	364	5.217	0.0130	4.999	3420
ST2672.3C-duplicate	2.04	0.365	0.004	0.005	b.d.	0.031	0.126	571	5.469	0.0083	5.126	3940
BA2372 (granite)	2.03	0.018	0.022	0.002	b.d.	0.019	b.d.	3.85	0.1569	0.0003	0.1546	22
Impact-melt rocks (clasts in suevitic breccia)												
ST2440.8C	0.96	1.07	0.928	–	–	–	–	5.57	0.1521	0.0004	0.1487	17.3
ST2440.8C-duplicate	0.54	0.717	0.682	0.466	1.56	10.4	6.29	5.08	0.1511	0.0003	0.1480	16.8
ST2453.3C	0.99	0.643	0.711	–	–	–	–	4.37	0.1554	0.0002	0.1528	20.6
ST2453.3C-duplicate	1.36	0.711	0.435	0.338	1.32	6.82	8.73	7.91	0.1565	0.0002	0.1517	20
ST2470.6C	0.96	0.120	0.514	0.197	0.502	2.57	3.20	1.13	0.1634	0.0002	0.1628	28.4
ST2470.6C-duplicate	0.52	0.120	0.314	0.182	0.390	3.69	3.82	1.86	0.1648	0.0004	0.1636	29.1
ST2565.0C	1.43	0.637	0.058	0.033	0.105	0.667	0.695	55.1	0.5181	0.0009	0.4850	283
ST2567.6C	0.11	0.264	0.419	0.115	0.449	2.42	1.57	3.07	0.2038	0.0004	0.2019	59.3
ST2570.0C	1.00	0.278	0.312	–	–	–	–	4.34	0.2234	0.0004	0.2208	74.2
ST2570.0C-duplicate	0.96	0.286	0.171	0.098	0.312	1.95	2.74	8.16	0.2296	0.0004	0.2247	77.3
ST2582.1C	0.21	0.562	0.445	0.216	1.02	9.13	8.43	6.13	0.1880	0.0003	0.1843	45.4
Breccias that contain impact-melt rock												
ST2562.8C	1.00	0.655	0.156	0.077	0.205	1.32	1.42	20.8	0.3451	0.0004	0.3327	162
ST2570.9C	1.24	1.14	0.149	0.113	0.565	4.24	6.52	38.2	0.4190	0.0007	0.3961	212
Reworked impact-melt clast												
UN749.4	2.01	0.312	0.007	0.006	0.015	0.186	0.187	259	1.662	0.0028	1.507	1090

[a]Sample localities and depths are in Table 1.

[b]$\gamma_{Os(T=36Ma)}$ = percent deviation of $^{187}Os/^{188}O$ from chondritic average at time of comparison, T = 36 Ma.

[c]b.d. = below detection.

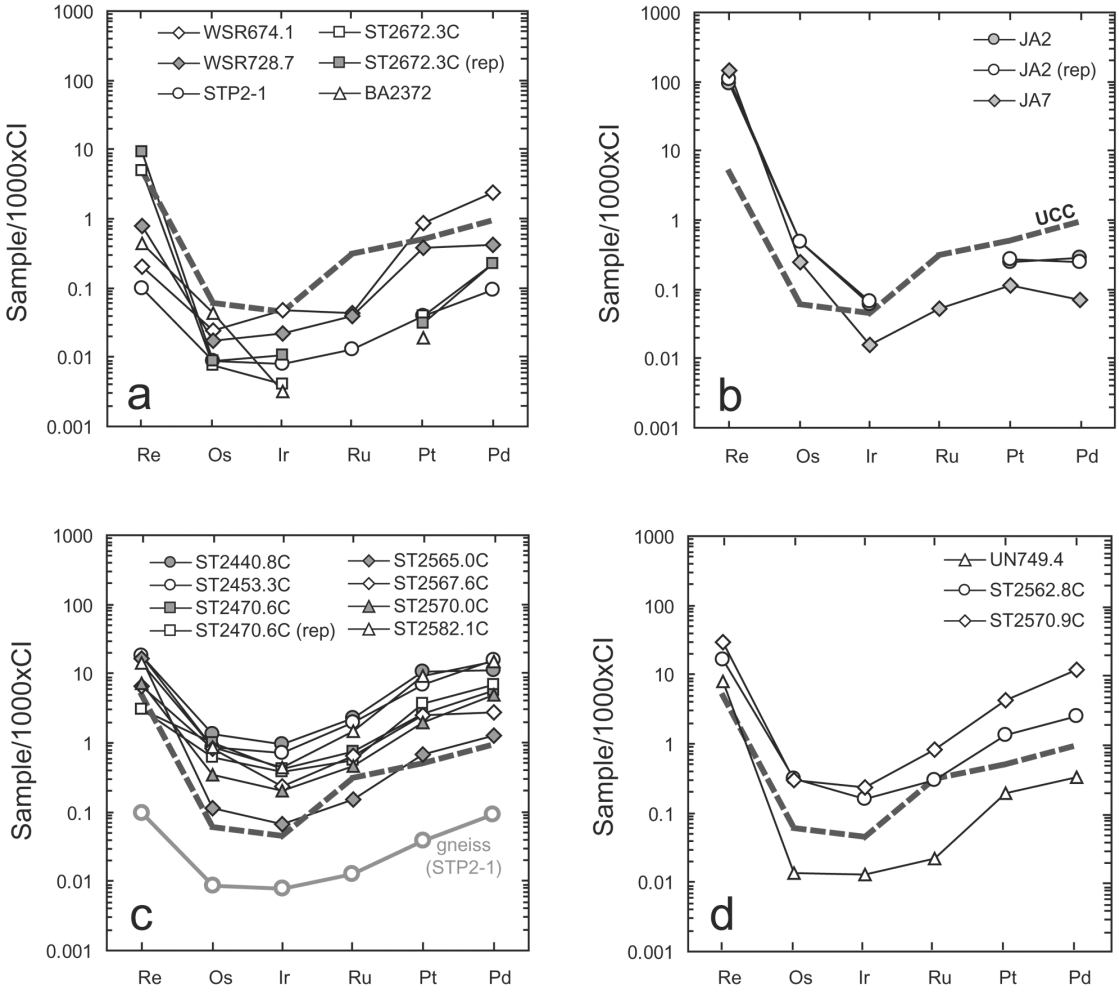

Fig. 2. Chondrite-normalized Re-PGE pattern (CI values from Palme and Jones [2003]). a) Target crystalline basement rocks (pre-Mesozoic) and nonmarine sediments (Cenozoic). b) Target marine sediments (Tertiary). c) Impact-melt rocks. d) Breccias that contain impact-melt rock and a reworked impact-melt clast. For comparison, Re and PGE abundances of average upper continental crust (UCC) are also plotted as the dashed line (UCC values from Peucker-Ehrenbrink and Jahn [2001]).

0.2247 (γ_{Os} = +16.8 to +59.3) (Table 2). The PGE pattern for sample ST2565.0C is similar to other impact-melt rocks, but its absolute concentrations are the lowest of the impact-melt rocks, and its $^{187}Re/^{188}Os$ of 55.1 is significantly higher. Its initial $^{187}Os/^{188}Os$ of 0.485 (γ_{Os} = +283) is also significantly higher than that of the other impact-melt rocks.

Samples of breccia that contain impact-melt rock (ST2562.8C and ST2570.9C) are natural mixtures that also contain abundant fragments of target-derived quartzofeldspathic gneiss similar to sample STP2-1 and sparse fragments of metamafic rock similar to sample ST2672.3C. Sample ST2562.8 is a suevitic breccia in which impact-melt particles are less abundant than target-rock fragments, whereas ST2570.9 is mostly (>50%) melt that contains abundant target-rock fragments (Table 1). The $^{187}Re/^{188}Os$ ratios (20.8 and 38.2) of these breccias are higher than those of all the impact-melt rocks except for the anomalous, low-Os sample ST2565.0C, but within the range of target-rock fragments in the breccia (e.g., STP2-1 and ST2672.3C). The initial $^{187}Os/^{188}Os$ ratios (0.3451 and 0.4190, γ_{Os} = +162 and +212) of these breccias are higher than those of all impact-melt rocks except low-Os sample ST2565.0C, but lower than those of most target materials including STP2-1 and ST2672.3C. These relations are consistent with the character of the breccias as natural mixtures of impact melt and target rock fragments. Concentrations of PGE in these breccias are higher than in the target rocks contained as fragments (e.g., STP2-1, ST2672.3C), but similar to concentrations in most of the impact-melt rocks (Table 2), suggesting that a significant proportion of the PGE are derived from the impact melt. Except for the relative Re enrichments, the chondrite-normalized PGE patterns of these breccias (Fig. 2d) are also similar to those of the impact-melt rocks (Fig. 2c).

One reworked impact-melt clast (sample UN749.4) was separated from a sedimentary-clast breccia. The PGE

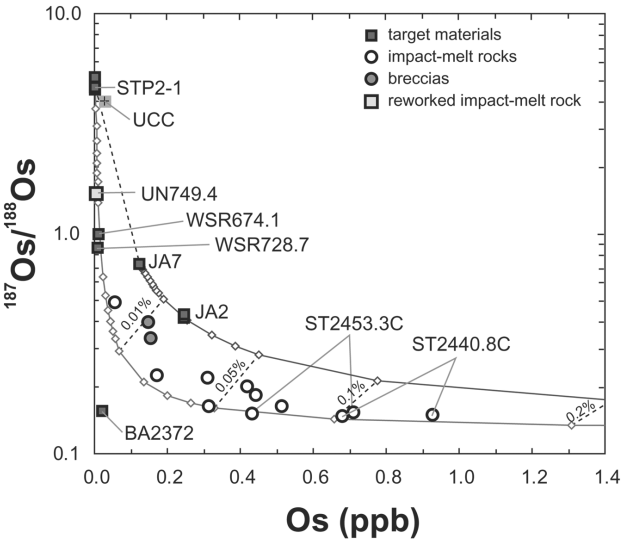

Fig. 3. Plot of $^{187}Os/^{188}Os$ versus Os concentration (in ppb). The curves show mixing between two target materials (STP2-1 and JA7) and a projectile of carbonaceous chondrite composition with Os = 653 ppb and $^{187}Os/^{188}Os$ = 0.126 (γ_{Os} = 0). For comparison, Os concentration and $^{187}Os/^{188}Os$ of the UCC are also plotted (values after Peucker-Ehrenbrink and Jahn [2001]).

concentrations of this sample are substantially lower than those of the other impact-melt rocks, but are 2–3× higher than those of the basement gneiss (Table 2). Rhenium is markedly enriched in this sample compared to its relatively low PGE concentrations. The chondrite-normalized PGE pattern of sample UN749.4 (Fig. 2d) is similar to those of the two breccias that contain impact-melt rock (samples ST2562.8C and ST2570.9C) and the low-Os impact-melt rock (sample ST2565.0C) but differs in having PGE concentrations lower than average UCC. The $^{187}Re/^{188}Os$ ratio of 1.66 is much higher than those of any other impact-melt rocks, and the initial $^{187}Os/^{188}Os$ ratio of 1.507 (γ_{Os} = +1090) is considerably more radiogenic than the other impact-melt rocks and even some of the crustal rocks and sediments.

DISCUSSION

Osmium Isotopic Evidence for a Meteoritic Component in Impact-Melt Rocks

Despite the enrichment of PGE in the impact-melt rocks compared to potential target materials investigated, the chondrite-normalized PGE patterns of the impact-melt rocks are highly nonchondritic, hence, the verification of a meteoritic component in the impact-melt rocks requires additional information. Modeling the relation between $^{187}Os/^{188}Os$ ratios and Os concentrations in impact melt rocks has proven to be a robust means of identifying meteoritic components and constraining the mass input from impactors in impact-melt rocks. This is due to the strong contrast in isotopic composition and concentration between typical crust and meteorites (e.g., Gelinas et al. 2004). We consider data for CBIS impact-melt rocks within the context of mixing between a chondritic component and most probable target components, such as the gneiss (sample STP2-1). We also chose sample JA7 as another crustal end-member for mixing calculations, because its high Os concentration could have had a supplemental effect on the Os budget of impact-melt rocks. The mixing model parameters used for the meteoritic component are: 653 ppb Os, $^{187}Os/^{188}Os$ = 0.126 (γ_{Os} = 0). These meteoritic parameters are consistent with the average composition of carbonaceous chondrites at 36 Ma (Walker et al. 2002; Horan et al. 2003).

The impact-melt rocks show a good fit to the calculated mixing curves generated for mixing between chondritic and crustal end members (Fig. 3). For this mixing model, the two samples with the lowest initial $^{187}Os/^{188}Os$ and the highest Os concentrations could have been produced by additions of 0.1–0.2% of a meteoritic component. Most other samples have compositions consistent with additions of 0.01–0.1% of a meteoritic component. The percentage of meteorite-derived Os contained in sample ST2440.8C could constitute as much as 70% of the total Os. However, a replicate analysis of the sample gives a meteoritic component of ~50%, indicating that the meteoritic component may have been unevenly mixed into the target materials, or given the small sample size, that these differences may reflect uneven distribution of PGEs due to a nugget effect. Using other chondrites as the end-member for mixing does not make a significant difference to the mixing calculations. For example, choosing values appropriate for an ordinary chondrite (728 ppb Os, $^{187}Os/^{188}Os$ = 0.128; Walker et al. 2002; Horan et al. 2003) results in only about 10% less of meteoritic component calculated for the impact-melt rocks (Fig. 3).

The proportions of meteoritic component in most impact-melt rocks of the CBIS are considerably lower than the estimates of 0.1–0.45 wt% (average 0.2 wt%) for impact-melt rocks of the Popigai crater (Tagle and Claeys 2005). On average, however, they are approximately a factor of 10 higher than those in impact-melt rocks of the Chicxulub impact crater (Gelinas et al. 2004). The lesser amount of meteoritic imprint on the Chicxulub impact-melt rocks is consistent with the general observation that larger impacts leave less of the meteoritic component by vaporizing and removing greater proportions of the projectile.

Rhenium and PGE Systematics in Impact-Melt Rocks

The Os isotopic data confirm substantial additions of extraterrestrial material to the impact-melt rocks, but nonchondritic elemental patterns indicate that the budgets of at least some PGE in the impact-melt rocks may have been dominated by target materials. An important clue to the nature of the target components in the impact-melt rocks is the Re/

Os ratio. The Re versus Os abundances and $^{187}Re/^{188}Os$ versus $^{187}Os/^{188}Os$ ratios of various impact-melt rocks and target materials are highly variable (Figs. 4a and 4b). All but sample ST2565.0C of the impact-melt rocks are characterized by relatively high Os and low Re contents ($^{187}Re/^{188}Os$ = 1.13–8.16), suggesting that the indigenous components in these samples are dominated by target material with relatively low Re/Os ratios (e.g., WSR674.1, WSR728.7, STP2-1, and BA2372), although it should be noted that all $^{187}Re/^{188}Os$ ratios are significantly higher than chondritic values ($^{187}Re/^{188}Os$ = ~0.4) (Walker et al. 2002). In contrast, one impact-melt rock (ST2565.0C), two breccias that contain impact-melt rock (ST2562.8C and ST2570.9C), and the reworked impact-melt rock (UN749.4) are enriched in Re relative to Os, and their $^{187}Re/^{188}Os$ ratios (20.8–259) trend towards the target rocks and sediments having high Re/Os (e.g., JA2, JA7, and ST2672.3C).

Among the low Re/Os target materials, the gneiss (STP2-1) is the most likely indigenous component in the impact-melt rocks, given that all of the impact-melt rocks come from suevitic crystalline-clast breccias that contain abundant fragments of this gneiss. However, assuming that projectile proportions of 0.01–0.1% were added to the gneiss, calculated mixtures have far less fractionated Re and PGE, than is actually observed in the impact-melt rocks (Fig. 5a). This may indicate that the gneiss cannot be the dominant, or at least sole, target component. Calculations for mixing between a chondritic projectile and several other possible target rocks can reproduce certain features of the Re and PGE patterns of the impact-melt rocks, but none of the single target materials can generate any of the impact-melt rocks by simple mixing (Figs. 5b–5e). For example, Re abundances in impact-melt rocks may be explained by the additions of high Re samples such as JA2 and JA7, but mixtures of the analyzed target materials and average UCC cannot reproduce the Ru, Pt, and Pd abundances of the impact-melt rocks.

In order to better characterize the indigenous component contained in the impact-melt rocks, variable proportions (0.01–0.1%) of the projectile component(s) are subtracted from the impact-melt rock with the highest Os concentration and lowest $^{187}Os/^{188}Os$ ratio (sample ST2440.8C). The calculated indigenous components have similar Re and PGE patterns, characterized by relative enrichment of Re, Ru, Pt, and Pd compared to Os and Ir (Fig. 6). The Re, Pt, and Pd abundances in the calculated indigenous components are little affected by the proportions of the projectile component in the impact-melt rock. In contrast, Os, Ir, and Ru abundances are highly dependent on the proportions of the projectile in the impact-melt rock. Because of the low Ir in most impact-melt rocks, the Ir abundance in the calculated indigenous component is especially sensitive to the proportion of projectile component. The subtraction of more than ~0.1% of the projectile component removes all Ir from the remaining target component. Thus, the maximum amount of the projectile that mixed with target materials to form the impact melts was probably no more than ~0.1%. This conclusion is consistent with the results of the previous mixing calculations based on Os isotopes for most samples of impact-melt rock. However, as noted earlier, the two samples with the lowest $^{187}Os/^{188}Os$ ratios and highest Os concentrations (ST2440.8C and ST2453.3C) could have been produced by additions of 0.1–0.2% of a meteoritic component.

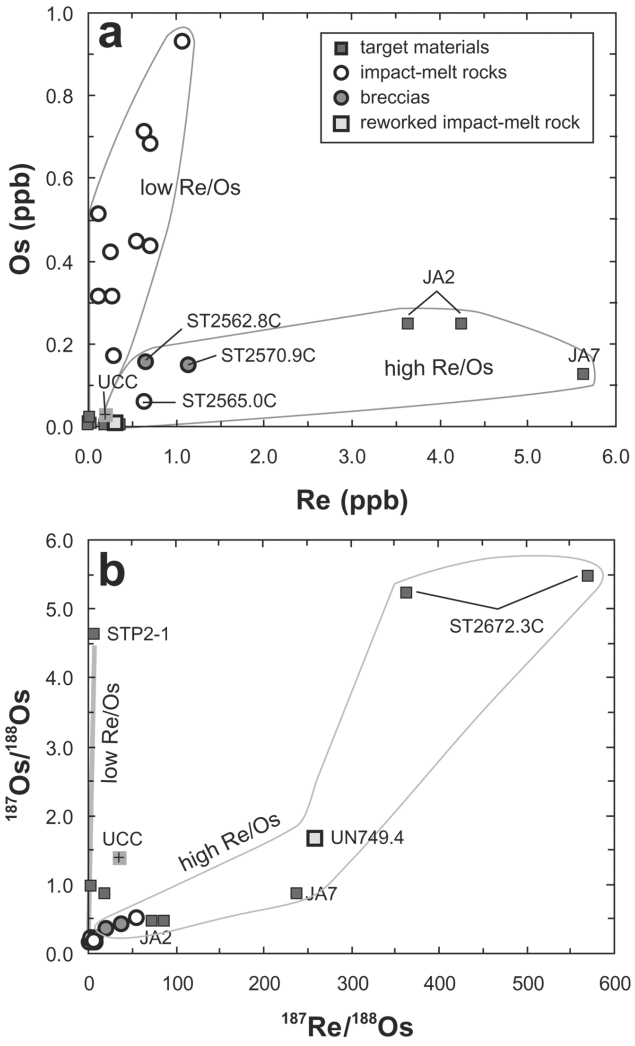

Fig. 4. Plots for impact-melt rocks and target materials. a) Concentrations of Re and Os (in ppb). b) $^{187}Re/^{188}Os$ versus $^{187}Os/^{188}Os$. Two of the breccias that contain impact-melt rock (ST2562.8C and ST2570.9C) and one impact-melt rock (ST2565.0C) with lowest Os concentration trend toward the target marine sediments of Tertiary age (JA2 and JA7) with high $^{187}Re/^{188}Os$.

Identification of Projectile Type

For unequivocal identification of a meteoritic component using PGE in impact-melt rocks, the indigenous PGE concentrations must be subtracted from the abundances found

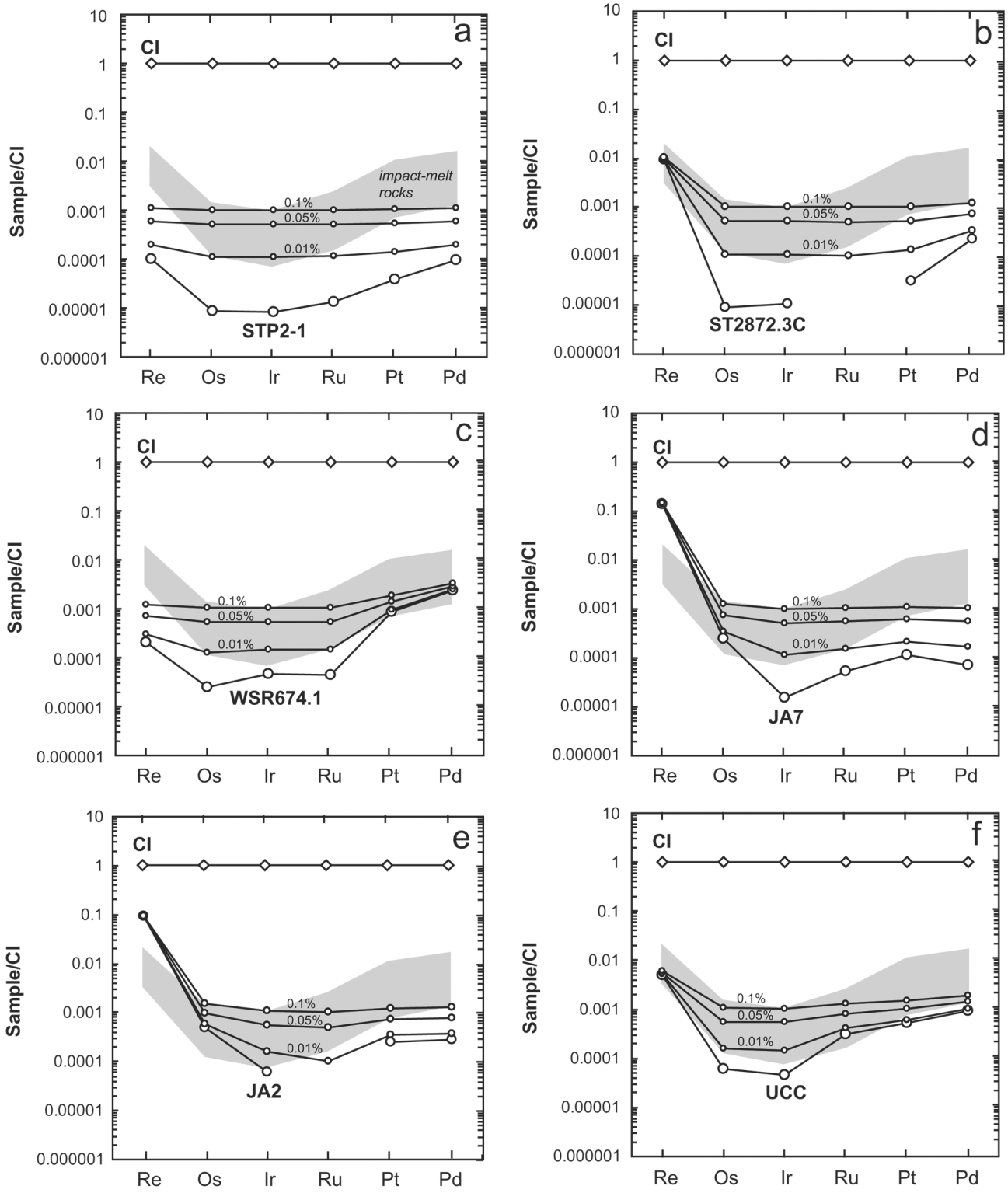

Fig. 5. Chondrite-normalized Re and PGE patterns for mixtures between a carbonaceous chondrite projectile and representative target materials. Target materials used in mixing calculations are a) quartzofeldspathic gneiss, STP2-1; b) brecciated metamafic rock, ST2672.3C; c) Cretaceous non-marine clay with the highest Pt and Pd concentrations, WSR674.1; d) Middle Eocene carbonate sediment with the highest Re abundance, JA7; e) upper Paleocene glauconite-bearing sand, JA2; and f) UCC average (after Peucker-Ehrenbrink and Jahn [2001]).

in the impact-melt rocks, so that the meteoritic abundance ratios can be determined (Koeberl and Shirey 1997; Koeberl 1998). Linear correlations of certain PGE abundances in suites of impact-melt rocks have been used to identify the projectile in several impact craters (e.g., Palme et al. 1978; Morgan et al. 1979; Evans et al. 1993; Schmidt et al. 1997; Tagle and Claeys 2005).

The interelemental correlations of PGE in the CBIS impact-melt rocks are shown in Fig. 7. The PGE do not correlate well with one another, nor are any of the interelemental ratios similar to chondritic. This prohibits decisive discrimination of the chemical nature of the projectile. Most of the elemental ratios of the impact-melt rocks are instead similar to those of certain target materials with low Re/Os and Os/Ir ratios, suggesting that the PGE budget within the impact-melt rocks is dominated by the target materials. There is no correlation between the elemental ratios and impact-melt rocks with the lowest $^{187}Os/^{188}Os$, which are interpreted to have the highest proportions of the projectile. For example, the elemental ratios for samples ST2440.8C and ST2453.3C, which have the lowest $^{187}Os/^{188}Os$ among the investigated impact-melt rocks, are very different from any known chondrite. At present, therefore, it is not possible to constrain the chemical nature of the projectile by the relative proportions of siderophile elements in the CBIS.

Origin of Non-Chondritic PGE Enrichments in Impact-Melt Rocks

The discrepancy in Re and PGE budgets between the calculated indigenous component and any of the potential target materials examined here may be explained by one or more of the following: 1) contamination by a projectile with nonchondritic relative abundances of Re and PGE, 2) contributions from as yet unsampled target materials, which in combination can match the calculated indigenous component, and/or 3) syn- to post-impact fractionations of the Re and PGE.

Some differentiated meteorites such as irons, stony-irons, and achondrites have fractionated PGE. For example, some iron meteorites, such as IVA irons, can have PGE patterns depleted in Os and Ir and enriched in Pt and Pd (Walker et al. 2005). However, the degree of Ru depletion relative to Pt and Pd (Ru/Pt = ~0.5–0.6) is not as prominent in the iron meteorites as observed in the impact-melt rocks (Ru/Pt = ~0.1–0.2). In addition, no known iron meteorites have Re/Os sufficiently fractionated to account for the impact-melt rock compositions. Achondrites generally have insufficient PGE to consider in mixing scenarios. Consequently, appealing to an impactor with the composition of a differentiated meteorite is unlikely to explain the nonchondritic PGE abundance patterns in the impact-melt rocks. We conclude that options (2) or (3), or a combination of both, are the most viable process to explain the observed PGE systematics of the impact-melt rocks.

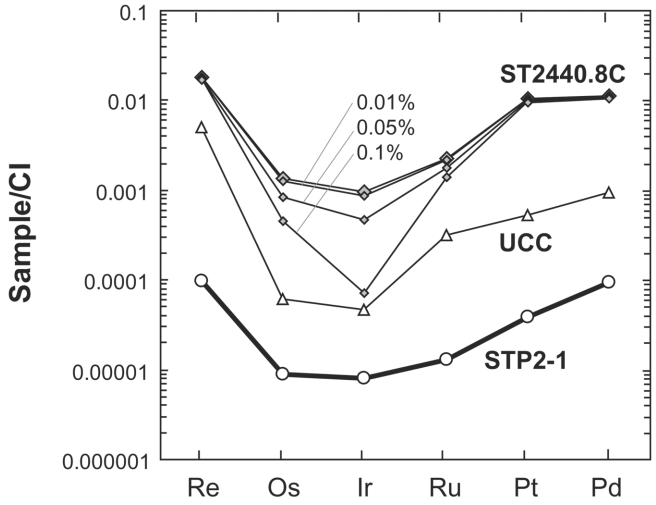

Fig. 6. Chondrite-normalized Re and PGE patterns of the hypothetical indigenous component in the impact-melt rock (ST2440.8C) derived by extracting variable (0.01–0.1%) amounts of a projectile with chondritic composition. Re and PGE patterns for UCC and gneiss sample STP2-1 are shown for reference.

Because a large impact event will affect a large volume of crustal materials, it is conceivable that the indigenous component in the impact-melt rocks was derived from a variety of target materials. The Re abundances of the calculated indigenous components may be balanced by additions of the highly Re-enriched uppermost sediments (e.g., JA2 and JA7). However, mixtures of the investigated target rocks cannot reproduce the enriched Pt and Pd abundances of the calculated indigenous components due to low Pt and Pd abundances in all of the target rocks. For example, the Re and PGE pattern of a mixture consisting of 50% each of JA7, which has the highest Re concentrations, and WSR674.1, which has the highest Pt and Pd concentrations of the investigated target materials, does not match that of the calculated indigenous component as shown in Fig. 8a. Further, the addition of gneiss (Fig. 8b) tends only to slightly dilute Re and PGE abundances of the hybrid mixtures, and does not change the general Re and PGE pattern. This suggests that addition of even 50% or more by mass of basement gneiss would little affect the Re and PGE abundances in the hybrid mixture. Finally, while certain combinations of target materials (e.g., ~17% JA2, ~17% WSR674.1, ~17% WSR728.7, and 50% STP2-1) can reproduce the Re abundance of the calculated indigenous component in the impact-melt rocks, they can not reproduce the PGE abundances (Fig. 8c).

These mixing calculations show that the Re abundance of the calculated indigenous component can be matched by addition of small amounts of Re-rich sedimentary materials in the hybrid mixtures of target materials. However, the PGE,

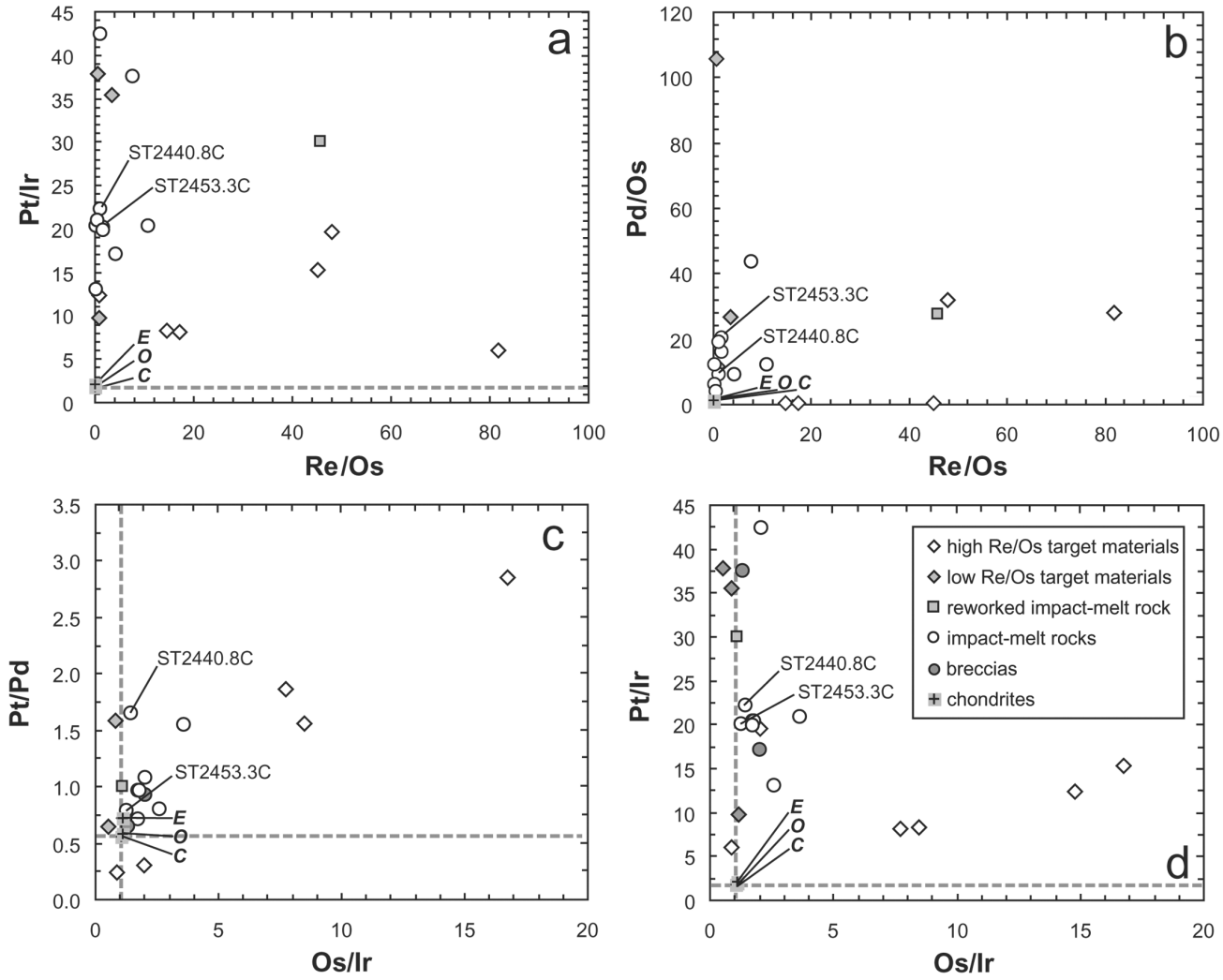

Fig. 7. PGE ratios of the impact-melt rocks and target materials: a) Pt/Ir versus Re/Os; b) Pd/Os versus Re/Os; c) Pt/Pd versus Os/Ir; d) Pt/Ir versus Os/Ir. Interelemental ratios for the impact-melt rocks show higher degree of variations compared to those of the three main groups of chondrites, prohibiting decisive discrimination of the chemical nature of the projectile. The most projectile-rich melt rocks (ST2440.8C and ST2453.3C) have PGE ratios that differ from any known chondrite. Average carbonaceous (C), ordinary (O), and enstatite (E) chondrite values are from Horan et al. (2003). Dotted lines are interelemene carbonaceous chondrite.

especially Ru, Pt, and Pd abundances are factors of 10–45× more enriched in the calculated indigenous component than is observed in any combination of target materials. Certain terrestrial materials such as S-undersaturated continental flood basalts, black shales, and hydrogenetic manganese crusts can have enriched PGE, especially Pt and Pd abundances (Kramar et al. 2001), and the presence of such materials, if formed in the target region, might explain the enriched PGE abundances of the impact-melt rocks. However, the PGE abundances of metamafic rock sample ST2672.3C are well below those of the overlying sedimentary units (Table 2 and Fig. 2b). Dark gray carbonaceous clays in the Cretaceous Potomac Formation (Powars and Bruce 1999; Powars 2000) are a minor but potentially significant target component that was not analyzed in this study. Analyses of additional target materials may be needed to determine if unusual crustal materials high in PGE, especially Pt and Pd, could have significantly contributed to the impact-melt.

Terrestrial impact events generally are open system processes, and they can, in some cases, cause fractionation of the primary PGE signatures of the projectile (Gibbons et al. 1976; Mittlefehldt et al. 1992; Evans and Chai 1997; Lee et al. 2003). Fractionation processes at the initial stage of the impact event may include vaporization/condensation and variable oxidation within the ejecta cloud, resulting in the selective incorporation of condensed PGE into impact melt. For example, Ru/Ir ratios of ejecta layers are positively correlated with distance from the Chicxulub impact structure (Evans et al. 1993), consistent with the volatility controlled fractionation between Ir and Ru. In the impact-melt rocks of

the CBIS, however, the more volatile elements Ru, Pt, and Pd are more enriched than the more refractory elements Os and Ir, excluding the possibility of volatility control on PGE fractionation. At present, it is difficult to consider the effects of other fractionation processes on PGE signatures, because little is known about those processes.

Fractionation processes related to post-impact hydrothermal activity also may be important. The degree of PGE mobilization within marine systems (e.g., CBIS) may exceed that at continental sites (e.g., Popigai) (Evans et al. 1993; Lee et al. 2003), given the solubility of some PGE in seawater. The impact-melt rocks sampled in this study are from clasts in a suevitic crystalline-clast breccia that shows petrographic evidence for pervasive hydrothermal chloritization and albitization (Horton et al. 2004, 2005b; Sanford 2005). However, the PGE abundances in felsic and mafic blocks from this breccia (STP2-1 and ST2672.3C) could not have provided a direct source for a hydrothermal fluid to have selectively scavenged Pt and Pd and precipitated them in the impact-melt rocks. Alternatively, the PGE budget in the impact-melt rocks may be partly attributed to Pt and Pd scavenged from overlying sedimentary sequences (e.g., WSR674.1) having higher Pt and Pd abundances than the basement rocks. The new results for the CBIS suggest that projectile-target mixing was a complex process, but the mechanisms for enrichment and fractionation of PGE in the impact-melt rocks are undetermined. Despite the complexity, the results indicate that the PGE budgets of the CBIS impact-melt rocks are dominated by the target materials rather than the projectile. In addition, the enriched Pt and Pd abundances in the impact-melt rocks may have largely originated from mixing or other processes within the target materials rather than from additions of extraterrestrial material.

CONCLUSIONS

The PGE concentrations of impact-melt rocks in suevitic crystalline-clast breccia from the CBIS are enriched relative to most of the investigated target rocks, suggesting substantial addition of a meteoritic component. Os, Ir, and Ru abundances in the impact melt rocks are highly dependent on the proportions of the projectile whereas the Re, Pt, and Pd abundances are little affected.

Because the PGE abundances in the impact-melt rocks are dominated by the target materials, all of the interelemental ratios of the impact-melt rocks are nonchondritic. At present, the chemical nature of the projectile cannot be constrained by the relative proportions of siderophile elements. Therefore, it remains unclear whether the Late Eocene Chesapeake Bay impact event is related to a comet or asteroid shower.

The proportions of the projectile contained in the target rocks, permitted by the PGE mixing models, are 0.01–0.1% by mass. However, the percentage of meteorite-derived Os could constitute as much as 70% for an impact-melt rock with the highest Os concentration. The proportions of meteoritic

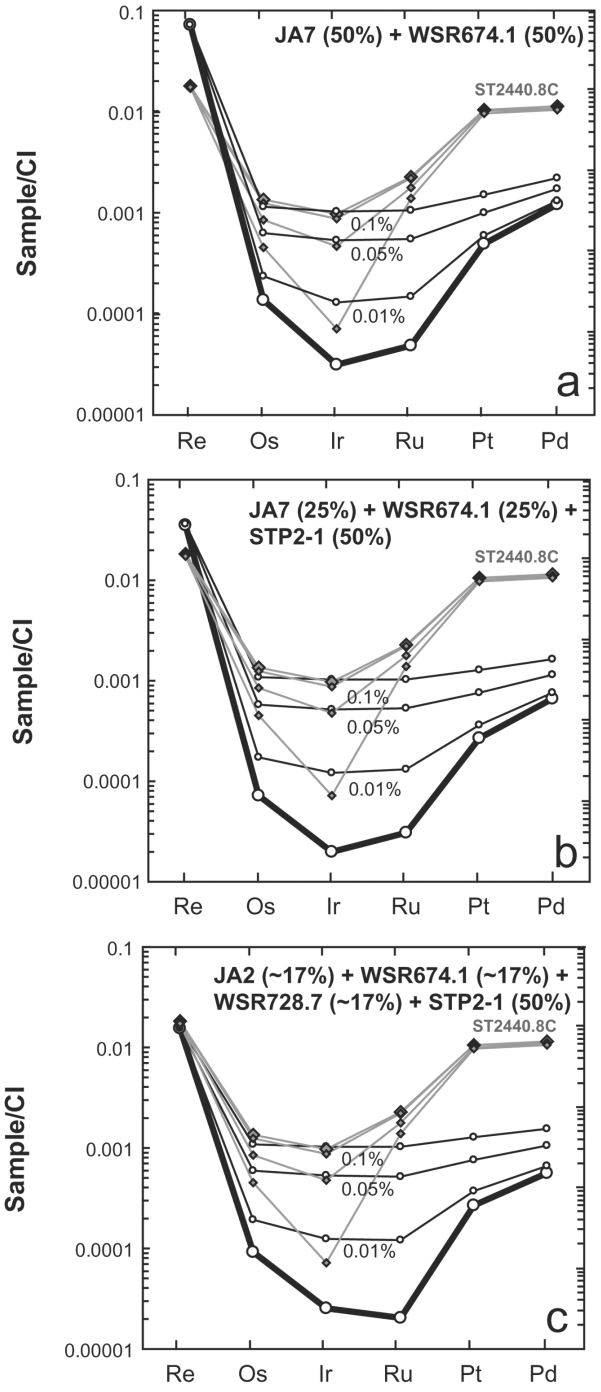

Fig. 8. Chondrite-normalized Re and PGE patterns of hybrid mixtures of target materials. The hypothetical indigenous component derived from the impact-melt rock (ST2440.8C) is also shown for comparison: a) mixture consisting of 50% JA7 and 50% WSR674.1; b) mixture consisting of 50% STP2-1, 25% JA7 and 25% WSR674.1; and c) mixture consisting of ~17% JA2, ~17% WSR674.1, ~17% WSR728.7 and 50% STP2-1. The addition of gneiss (e.g., STP2-1) tends to slightly dilute PGE abundances of the mixture between JA7 and WSR674.1, but does not affect relative PGE abundances. Because of low Ru, Pt, and Pd abundances in all of the examined target rocks, no single target material or combination of target materials can reproduce the calculated indigenous component in the impact-melt rock.

component in the impact-melt rocks of the CBIS are about 10× higher than those in the Chicxulub crater (Gelinas et al. 2004) but lower than in the Popigai crater (Tagle and Claeys 2005).

The additions of 0.01–0.1% of a projectile component to any of the examined target materials result in nearly chondritic relative PGE abundances, which is in contrast to the distinctly nonchondritic PGE patterns of all impact-melt rocks. This discrepancy between model calculations and the observed compositions requires either 1) participation of unsampled target materials with high PGE, especially Pt and Pd abundances, or 2) syn- to post-impact PGE fractionation processes. Because of the lack of geological evidence for the presence of unusually PGE enriched target materials, the fractionations of PGE in the impact-melt rocks are considered to be results of impact-related processes. Among many of the viable processes, the endogenous enrichments of PGE, scavenged largely from the target materials by lower temperature processes such as the hydrothermal activity, are preferred to PGE fractionation occurring during the high temperature impact event by processes such as vaporization and condensation.

Acknowledgments–USGS investigations of the Chesapeake Bay impact structure are conducted in cooperation with the Hampton Roads Planning District Commission and the Virginia Department of Environmental Quality. The USGS provided funds for drilling the Cape Charles Sustainable Technology Park test hole and studies of the drill core. The Re-Os and PGE analyses for this study were supported by NASA Grant NNG04GK52G (to R. J. W.). We thank Melissa A. Berke, Christian Koeberl, Klaus J. Schulz, and an anonymous reviewer for constructive reviews that significantly improved the paper.

Editorial Handling—Dr. John Spray

REFERENCES

Bodiselitsch B., Montanari A., Koeberl C., and Coccioni R. 2004. Delayed climate cooling in the Late Eocene caused by multiple impacts: High-resolution geochemical studies at Massignano, Italy. *Earth and Planetary Science Letters* 223:283–302.

Bottomley R. J., Grieve R. A. F., York D., and Masaitis V. 1997. The age of the Popigai impact event and its relation to events at the Eocene/Oligocene boundary. *Nature* 388:365–368.

Colodner D. C., Boyle E. A., Edmond J. M., and Thompson J. 1992. Post-depositional mobility of platinum, iridium, and rhenium in marine sediments. *Nature* 358:402–404.

Esser B. K. and Turekian K. K. 1993. The osmium isotopic composition of the continental crust. *Geochimica et Cosmochimica Acta* 57:3093–3104.

Evans N. J. and Chai C. F. 1997. The distribution and geochemistry of platinum-group elements as event markers in the Phanerozoic. *Paleogeography, Paleoclimatology, Paleoecology* 132:373–390.

Evans N. J., Gregoire D. C., Goodfellow W. D., McInnes B. I., Miles N., and Veizer J. 1993. Ru/Ir ratios at the Cretaceous-Tertiary boundary: Implications for PGE source and fractionation within the ejecta cloud. *Geochimica et Cosmochimica Acta* 57:3149–3158.

Farley K. A., Montanari A., Shoemaker E. M., and Shoemaker C. S. 1998. Geochemical evidence for a comet shower in the Late Eocene. *Science* 280:1250–1253.

Gelinas A., Kring D. A., Zurcher L., Urrutia-Fucugauchi J., Morton O., and Walker R. J. 2004. Osmium isotope constraints on the proportion of projectile component in Chicxulub impact-melt rocks. *Meteoritics & Planetary Science* 39:1003–1008.

Gibbons R. V., Hörz F., Thompson T. D., and Brownlee D. E. 1976. Metal spherules in Wabar, Monturaqui, and Henbury impactites. Proceedings, 7th Lunar Science Conference. pp. 863–880.

Grieve R. A. F. 1991. Terrestrial impact: The record in the rocks. *Meteoritics* 26:175–194.

Horan M. F., Walker R. J., Morgan J. W., Grossman J. N., and Rubin A. E. 2003. Highly siderophile elements in chondrites. *Chemical Geology* 196:5–20.

Horton J. W., Jr. and Izett G. A. 2005. Crystalline-rock ejecta and shocked minerals of the Chesapeake Bay impact structure, USGS-NASA Langley core, Hampton, Virginia, with supplemental constraints on the age of impact. In *Studies of the Chesapeake Bay impact structure—The USGS-NASA Langley corehole, Hampton, Virginia, and related coreholes and geophysical surveys,* edited by Horton J. W., Jr., Powars D. S., and Gohn G. S. Washington, D.C.: U.S. Geological Survey. pp. E1–E30.

Horton J. W., Jr., Kunk M. J., Naeser C. W., Naeser N. D., Aleinikoff J. N., and Izett G. A. 2002. Petrography, geochronology, and significance of crystalline basement rocks and impact-derived clasts in the Chesapeake Bay impact structure, southeastern Virginia (abstract). *Geological Society of America Abstracts with Programs* 34:466.

Horton J. W., Jr., Gohn G. S., Powars D. S., Jackson J. C., Self-Trail J. M., Edwards L. E., and Sanford W. E. 2004. Impact breccias of the central uplift, Chesapeake Bay impact structure: Initial results of a test hole at Cape Charles, Virginia (abstract). *Geological Society of America Abstracts with Programs* 36: 266.

Horton J. W., Jr., Aleinikoff J. N., Kunk M. J., Gohn G. S., Edwards L. E., Self-Trail J. M., Powars D. S., and Izett G. S. 2005a. Recent research on the Chesapeake Bay impact structure, USA: Impact debris and reworked ejecta. In *Large meteorite impacts III,* edited by Kenkmann T., Hörz F., and Deutsch A. Boulder, Colorado: Geological Society of America. pp. 147–170.

Horton J. W., Jr., Gohn G. S., Jackson J. C., Aleinikoff J. N., Sanford W. E., Edwards L. E., and Powars D. S. 2005b. Results from a scientific test hole in the central uplift, Chesapeake Bay impact structure, Virginia, USA (abstract #2003). 36th Lunar and Planetary Science Conference. CD-ROM.

Horton J. W., Jr., Powars D. S., and Gohn G. S. 2005c. Studies of the Chesapeake Bay impact structure—Introduction and discussion. In *Studies of the Chesapeake Bay impact structure—The USGS-NASA Langley corehole, Hampton, Virginia, and related coreholes and geophysical surveys,* edited by Horton J. W., Jr., Powars D. S., and Gohn G. S. Washington, D.C.: U.S. Geological Survey. pp. A1–A24.

Koeberl C. 1998. Identification of meteoritical components in impactites. In *Meteorites: Flux with time and impact effects,* edited by Grady M. M., Hutchison R., McCall G. J. H., and Rothery D. A. London: The Geological Society. pp. 133–152.

Koeberl C. and Shirey S.B. 1993. Detection of a meteoritic component in Ivory Coast tektites with rhenium-osmium isotopes. *Science* 261:595–598.

Koeberl C., Poag C. W., Reimold W. U., and Brandt D. 1996. Impact origin of the Chesapeake Bay structure and the source of the North American tektites. *Science* 271:1263–1266.

Koeberl C. and Shirey S. B. 1997. Re-Os isotope systematics as a diagnostic tool for the study of impact craters and distal ejecta. *Paleogeography, Paleoclimatology, Paleoecology* 132:25–46.

Koeberl C., Peucker-Ehrenbrink B., Reimold W. U., Shukolyukov A., and Lugmair G. W. 2002. A comparison of the osmium and chromium isotopic methods for the detection of meteoritic components in impactites: Examples from the Morokweng and Vredefort impact structures, South Africa. In *Catastrophic events and mass extinctions: Impacts and beyond,* edited by Koeberl C. and MacLeod K. G. Boulder Colorado, Geological Society of America. pp. 607–617.

Koeberl C., Farley K. A., Peucker-Ehrenbrink B., and Sephton M. A. 2004. Geochemistry of the end-Permian extinction event in Austria and Italy: No evidence for an extraterrestrial component. *Geology* 32:1053–1056.

Kramar U., Stüben D., Berner Z., Stinnesbeck W., Philipp H., and Keller G. 2001. Are Ir anomalies sufficient and unique indicators for cosmic events? *Planetary and Space Science* 49:831–837.

Lee C.-T., Wasserburg G. J., and Kyte F. T. 2003. Platinum-group elements (PGE) and rhenium in marine sediments across the Cretaceous-Tertiary boundary: Constraints on Re-PGE transport in the marine environment. *Geochimica et Cosmochimica Acta* 67:655–670.

Masaitis V. L., Danilin A. N., Mastchak M. S., Raikhlin T. V., and Selivanovskaya E. M. 1980. *Geology of astroblems.* Moscow: Nedra Press. 231 p.

Meisel T., Krähenbühl U., and Nazarov M. A. 1995. Combined osmium and strontium isotopic study of the Cretaceous-Tertiary boundary at Sumbar, Turkmenistan: A test for an impact vs. volcanic hypothesis. *Geology* 23:313–316.

Mittlefehldt D. W., See T. H., and Hörz F. 1992. Dissemination and fractionation of projectile materials in the impact melts from Wabar crater, Saudi Arabia. *Meteoritics* 27:361–370.

Morgan J. W. and Lovering J. F. 1967. Rhenium and osmium abundances in some igneous and metamorphic rocks. *Earth and Planetary Science Letters* 3:219–224.

Morgan J. W., Janssens M. J., Hertongen H., Gros H., and Takahashi H. 1979. Ries impact crater: Search for meteoritic material. *Geochimica et Cosmochimica Acta* 43:803–815.

O'Keefe J. D. and Ahrens T. J. 1987. Impact crater maximum depth of penetration and excavation (abstract). 18th Lunar and Planetary Science Conference. pp. 744–745.

Palme H. and Jones A. 2003. Solar system abundances of the elements. In *Meteorites, comets, and planets*, edited by Holland H. D. and Turekian K. K. New York: Elsevier. pp. 41–61.

Palme H., Gobel E., and Grieve R. A. F. 1979. The distribution of volatile and siderophile elements in the impact melt of East Clearwater (Quebec). Proceedings, 10th Lunar and Planetary Science. pp. 2465–2492.

Palme H., Janssens M. J., Takahashi H., Anders E., and Hertogen J. 1978. Meteoritic materials at five large craters. *Geochimica et Cosmochimica Acta* 42:313–323.

Palme H., Grieve R. A. F., and Wolf R. 1981. Identification of the projectile at the Brent crater, and further considerations of projectile types at terrestrial craters. *Geochimica et Cosmochimica Acta* 45:2417–2424.

Peucker-Ehrenbrink B. and Jahn B.-M. 2001. Rhenium-osmium isotope systematics and platinum group element concentrations: Loess and the upper continental crust. *Geochemistry, Geophysics, Geosystems* 2, doi: 10.1029/2001GC000172.

Poag C. W., Koeberl C., and Reimold W. U. 2004. *The Chesapeake Bay impact crater—Geology and geophysics of a Late Eocene submarine impact structure.* New York: Springer-Verlag. 522 p.

Powars D. S. 2000. *The effects of the Chesapeake Bay impact crater on the geologic framework and the correlation of hydrogeologic units of southeastern Virginia, south of the James River.* Washington, D.C.: U.S. Geological Survey. 53 p.

Powars D. S. and Bruce T. S. 1999. *The effects of the Chesapeake Bay impact crater on the geological framework and correlation of hydrogeologic units of the lower York-James Peninsula, Virginia.* Washington, D.C.: U.S. Geological Survey. 82 p.

Sanford W. E. 2005. A simulation of the hydrothermal response to the Chesapeake Bay bolide impact. *Geofluids* 5:185–201.

Sanford W. E., Gohn G. S., Powars D. S., Horton J. W., Jr., Edwards L. E., Self-Trail J. M., and Morin R. H. 2004. Drilling the central crater of the Chesapeake Bay impact structure: A first look. *Eos* 85:369–384.

Sawlowicz Z. 1993. Iridium and other platinum-group elements as geochemical markers in sedimentary environments. *Paleogeography, Paleoclimatology, Paleoecology* 104:253–270.

Schmidt G., Palme H., and Kratz K.-L. 1997. Highly siderophile elements (Re, Os, Ir, Ru, Rh, Pd, Au) in impact-melts from three European impact craters (Saaksjarvi, Mien, and Dellen): Clues to the nature of the impacting bodies. *Geochimica et Cosmochimica Acta* 61:2977–2987.

Schmitz B., Peucker-Ehrenbrink B., Heilmann-Clausen C., Aberg G., Asaro F., and Lee C.-T. 2004. Basaltic explosive volcanism, but no comet impact, at the Paleocene-Eocene boundary: High-resolution chemical and isotopic records from Egypt, Spain and Denmark. *Earth and Planetary Science Letters* 225:1–17.

Shirey S. B. and Walker R. J. 1995. Carius tube digestion for low-blank rhenium-osmium analysis. *Analytical Chemistry* 67:2136–2141.

Tagle R. and Claeys P. 2004. Comet or asteroid shower in the Late Eocene? *Science* 305:492.

Tagle R. and Claeys P. 2005. An ordinary chondrite impactor for the Popigai crater, Siberia. *Goechimica et Cosmochimica Acta* 69: 2877–2889.

Walker R. J., Horan M. F., Morgan J. W., Becker H., Grossman J. N., and Rubin A. E. 2002. Comparative ^{187}Re-^{187}Os systematics of chondrites: Implications regarding early solar system processes. *Geochimica et Cosmochimica Acta* 66:4187–4201.

Walker R. J., McCoy T. J., Schulte R. F., McDonough W. F., and Ash R. D. 2005. $^{187}Re/^{188}Os$, $^{190}Pt/^{186}Os$ isotopic and highly siderophile element systematics of group IVA irons (abstract#1288). 36th Lunar and Planetary Science Conference. CD-ROM.

Whitehead J., Papanastassiou D. A., Spray J. G., Grieve R. A. F., and Wasserburg G. J. 2000. Late Eocene impact ejecta: Geochemical and isotopic connections with the Popigai impact structure. *Earth and Planetary Science Letters* 181:473–487.

Winzer S. R., Lum R. K. L., and Schuhmann S. 1976. Rb, Sr, and Strontium isotopic composition, K/Ar age and large ion lithophile trace element abundances in rock and glasses from the Wanapitei Lake impact structure. *Geochimica et Cosmochimica Acta* 40:51–57.

Wolf R., Woodrow A. B., and Grieve R. A. F. 1980. Meteoritic material at four Canadian impact craters. *Geochimica et Cosmochimica Acta* 44:1015–1022.